

SUPPLEMENTARY MATERIALS

Influence of the Pseudohalide Ligands on the SIM Behaviour of Four-Coordinate Benzylimidazole-Containing Cobalt(II) Complexes

A. Świtlicka^a, B. Machura^a, R. Kruszynski^b, J. Cano^{c,d}, L.M. Toma^c, F. Lloret^c, M. Julve^{*c}

^a *Department of Crystallography, Institute of Chemistry, University of Silesia, 9th Szkolna St., 40–006 Katowice, Poland, anna.switlicka@gmail.com*

^b *Department of X-ray Crystallography and Crystal Chemistry, Institute of General and Ecological Chemistry, Lodz University of Technology, Zeromskiego St. 116, 90-924 Łódź, Poland*

^c *Department of Química Inorgànica/Instituto de Ciencia Molecular (ICMol), Facultat de Química de la Universitat de València, C/ Catedrático José Beltrán 2, 46980 Paterna, València, Spain. E-mail: miquel.julve@uv.es*

^d *Fundació General de la Universitat de València (FGUV), Universitat de València, 96480 Paterna, València, Spain*

Figures:

Figure S1. X-ray powder diffraction pattern of **1** at room temperature, together with the calculated pattern from the single crystal data.

Figure S2. X-ray powder diffraction pattern of **2** at room temperature, together with the calculated pattern from the single crystal data.

Figure S3. X-ray powder diffraction pattern of **3** at room temperature, together with the calculated pattern from the single crystal data.

Figure S4. IR spectra of **1**.

Figure S5. IR spectra of **2**.

Figure S6. IR spectra of **3**.

Figure S7. The solid reflectance spectra UV-Vis (a) and NIR (b) of Co(II) complexes

Figure S8. Frequency dependence of the (left) out-of-phase (χ_M'') and (right) in-phase (χ_M') components of the ac susceptibility for **1** under an applied static field of $H_{dc} = 500$ G with a ± 5.0 G oscillating field at frequencies in the range 1000-10000 Hz.

Figure S9. Frequency dependence of the (left) out-of-phase (χ_M'') and (right) in-phase (χ_M') components of the ac susceptibility for **1** under an applied static field of $H_{dc} = 1000$ G with a ± 5.0 G oscillating field at frequencies in the range 1000-10000 Hz.

Figure S10. Frequency dependence of the (left) out-of-phase (χ_M'') and (right) in-phase (χ_M') components of the ac susceptibility for **1** under an applied static field of $H_{dc} = 2500$ G with a ± 5.0 G oscillating field at frequencies in the range 1000-10000 Hz.

Figure S11. Frequency dependence of the (left) out-of-phase (χ_M'') and (right) in-phase (χ_M') components of the ac susceptibility for **2** under an applied static field of $H_{dc} = 1000$ G with a ± 5.0 G oscillating field at frequencies in the range 1000-10000 Hz.

Figure S12. Frequency dependence of the (left) out-of-phase (χ_M'') and (right) in-phase (χ_M') components of the ac susceptibility for **2** under an applied static field of $H_{dc} = 2500$ G with a ± 5.0 G oscillating field at frequencies in the range 1000-10000 Hz.

Figure S13. Frequency dependence of the (left) out-of-phase (χ_M'') and (right) in-phase (χ_M') components of the ac susceptibility for **3** under an applied static field of $H_{dc} = 1000$ G with a ± 5.0 G oscillating field at frequencies in the range 1000-10000 Hz.

Figure S14. Frequency dependence of the (left) out-of-phase (χ_M'') and (right) in-phase (χ_M') components of the ac susceptibility for **3** under an applied static field of $H_{dc} = 2000$ G with a ± 5.0 G oscillating field at frequencies in the range 1000-10000 Hz.

Figure S15. Arrhenius plots for **1** under applied fields of (left) 1000 and (right) 2500 G.

Figure S16. Cole-Cole plots for **1** in the temperature range 2.0-2.6 K at the indicated frequencies and under applied fields of (top) 500, (middle) 1000 and (bottom) 2500 G.

Figure S17. Natural logarithm of the χ_M''/χ_M' ratio vs. $1/T$ for **2** under a dc magnetic field of 1000 G and a ± 5.0 G oscillating field at the indicated frequencies.

Figure S18. Natural logarithm of the χ_M''/χ_M' ratio vs. $1/T$ for **3** under dc magnetic fields of (left) 1000 and (right) 2000 G and a ± 5.0 G oscillating field at the indicated frequencies

Tables:

Table S1. Selected bond lengths [\AA] and angles [$^\circ$] for **1-3**

Table S2. UV-Vis-NIR data for compounds **1-3**.

Table S3. Short intra- and intermolecular contacts detected in structures **2** and **3**.

CShM allows to determine a distance between the real metal environment and the ideal polyhedron. Mathematically, CShM of the original structure (Q) is a normalized root-mean-square deviation from the referenced structure with the desired symmetry (P) and it is expressed by eqn (1)

$$S_Q(P) = \min \left[\frac{\sum_{i=1}^n |\vec{q}_i - \vec{p}_i|^2}{\sum_{i=1}^n |\vec{q}_i - \vec{q}_0|^2} \right] \times 100 \quad (1)$$

where, \vec{q}_i are N vectors that contain the $3N$ Cartesian coordinates of the problem structure Q , \vec{p}_i contain the coordinates of the ideal polyhedron P and \vec{q}_0 is the position vector of the geometric center that is chosen to be the same for the two polyhedra. The minimum is taken for all possible relative orientations in space, isotropic scaling, and for all possible pairings of the vertexes of the problem and reference polyhedra. The value $S_Q(P)$ tends to zero, when the polyhedron Q is close to the ideal one. The maximum allowed value $S_Q(P)$ is 100, although in practice the values found for severely distorted chemical structures are very rarely larger than 40. Generally, it is assumed that shape measures of less than 1.0 indicate minor distortions from the reference shape; values of up to 3.0 units indicate important distortions, but the reference shape provides still a good stereochemical description.

The geometry of structure Q , which is intermediate between two polyhedra T and P , can be described by its position along the minimal distortion path given by the *generalized polyhedral interconversion coordinate* $\varphi_{T \rightarrow P}^Q$. It is derived from the shape measure of structure Q relative to the initial shape of the path, T , according to following equation

$$\varphi_{T \rightarrow P}^Q = \frac{100}{\theta_{TP}} \arcsin\left(\frac{\sqrt{S_Q(T)}}{10}\right) \quad (2)$$

When the structure is coincident with T , $\varphi_{T \rightarrow P}^Q$ is zero, while for a structure coincident with the end point of the P path, it amounts to 100%. Structures along the path have intermediate $\varphi_{T \rightarrow P}^Q$ values that correspond to the portion of the covered path (in percentage).¹⁻³

1. J. Cirera, P. Alemany and S. Alvarez, *Chem. Eur. J.*, 2004, **10**, 190.
2. D. Casanova, J. Cirera, M. Lluell, P. Alemany, D. Avnir and S. Alvarez, *J. Am. Chem. Soc.*, 2004, **126**, 1755.
3. J. Cirera, E. Ruiz and S. Alvarez, *Inorg. Chem.*, 2008, **47**, 2871

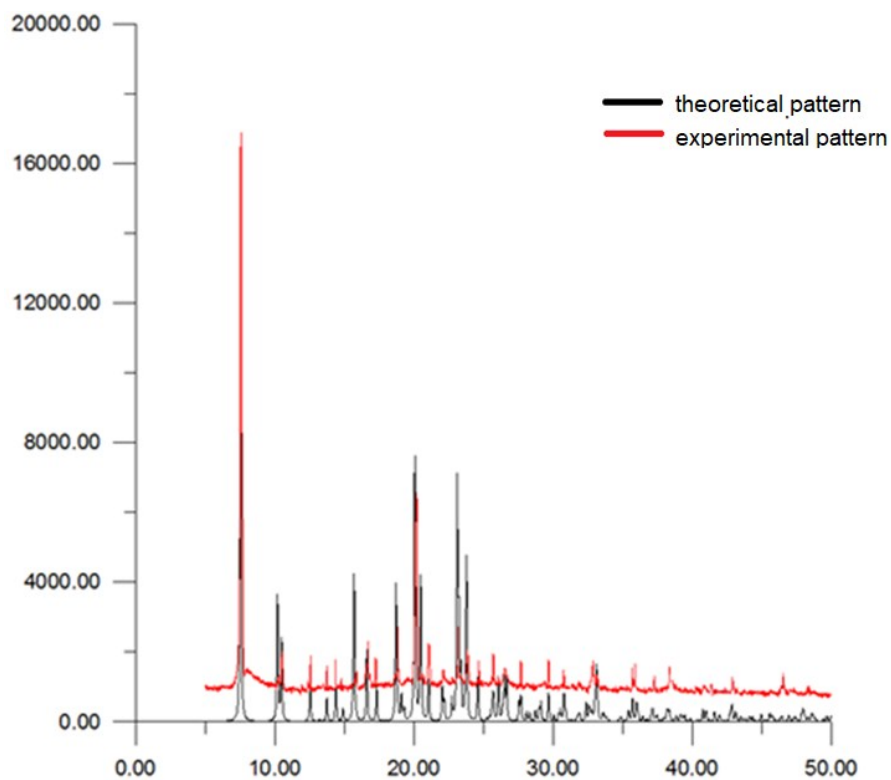


Figure S1. X-ray powder diffraction pattern of **1** at room temperature, together with the calculated pattern from the single crystal data.

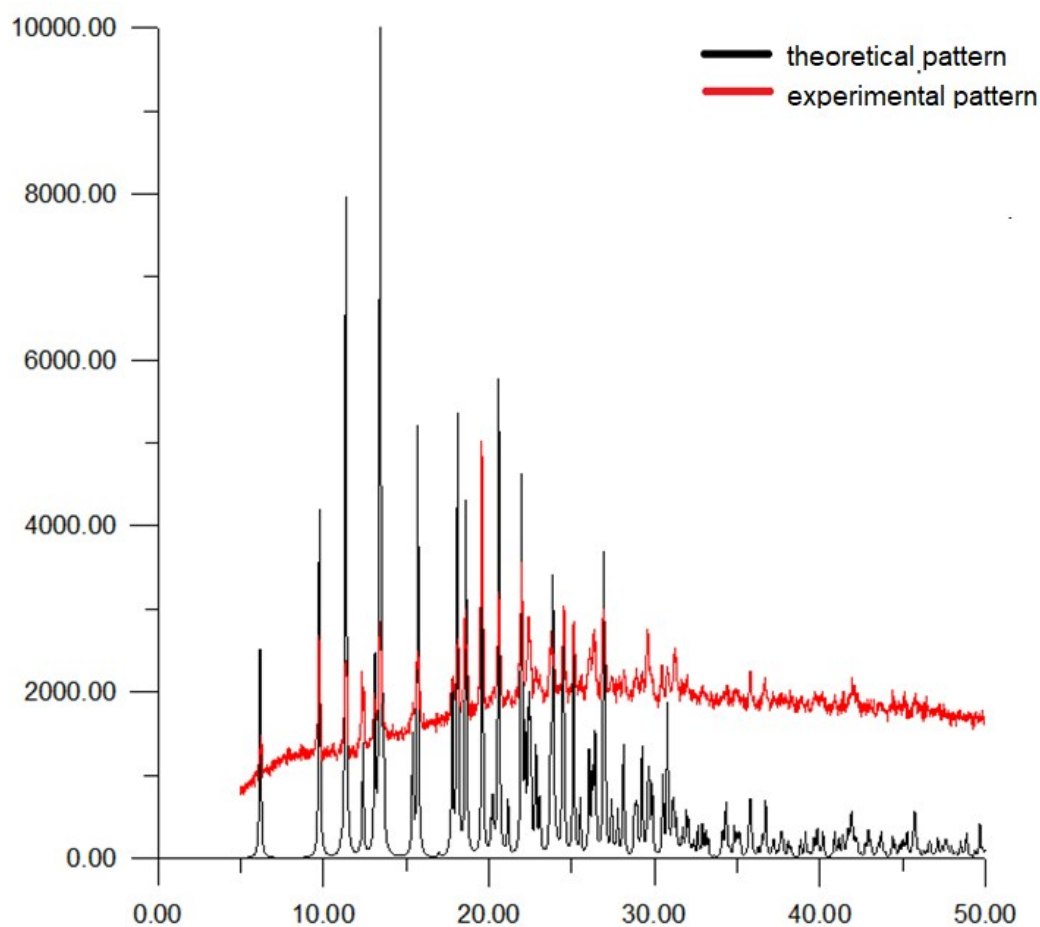


Figure S2. X-ray powder diffraction pattern of **2** at room temperature, together with the calculated pattern from the single crystal data.

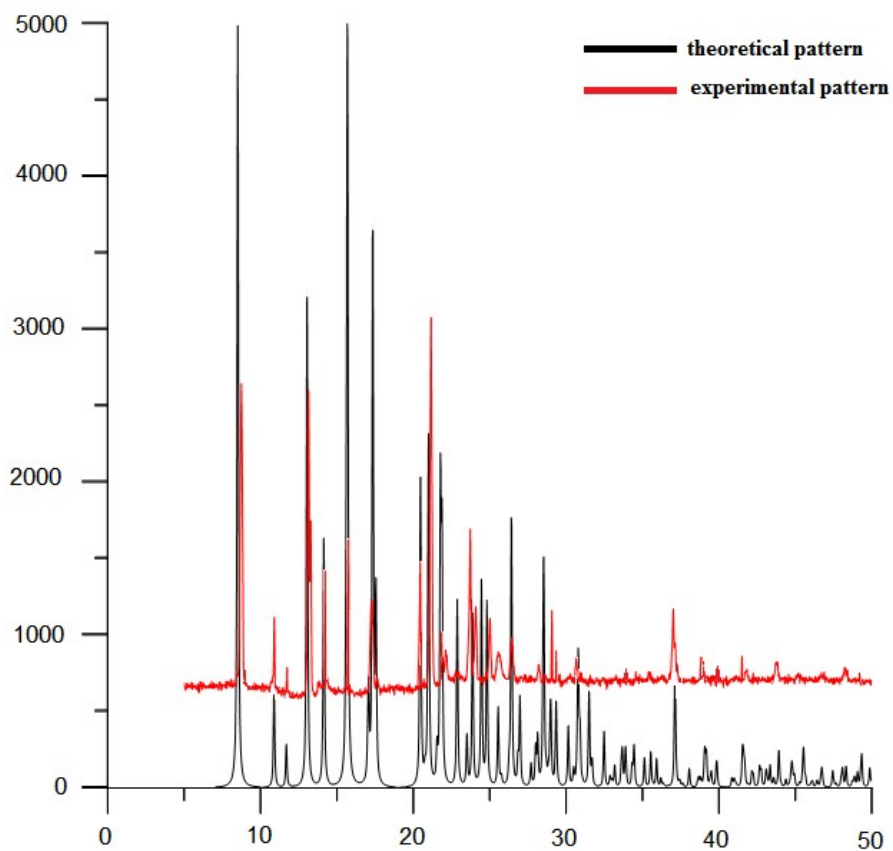


Figure S3. X-ray powder diffraction pattern of **3** at room temperature, together with the calculated pattern from the single crystal data.

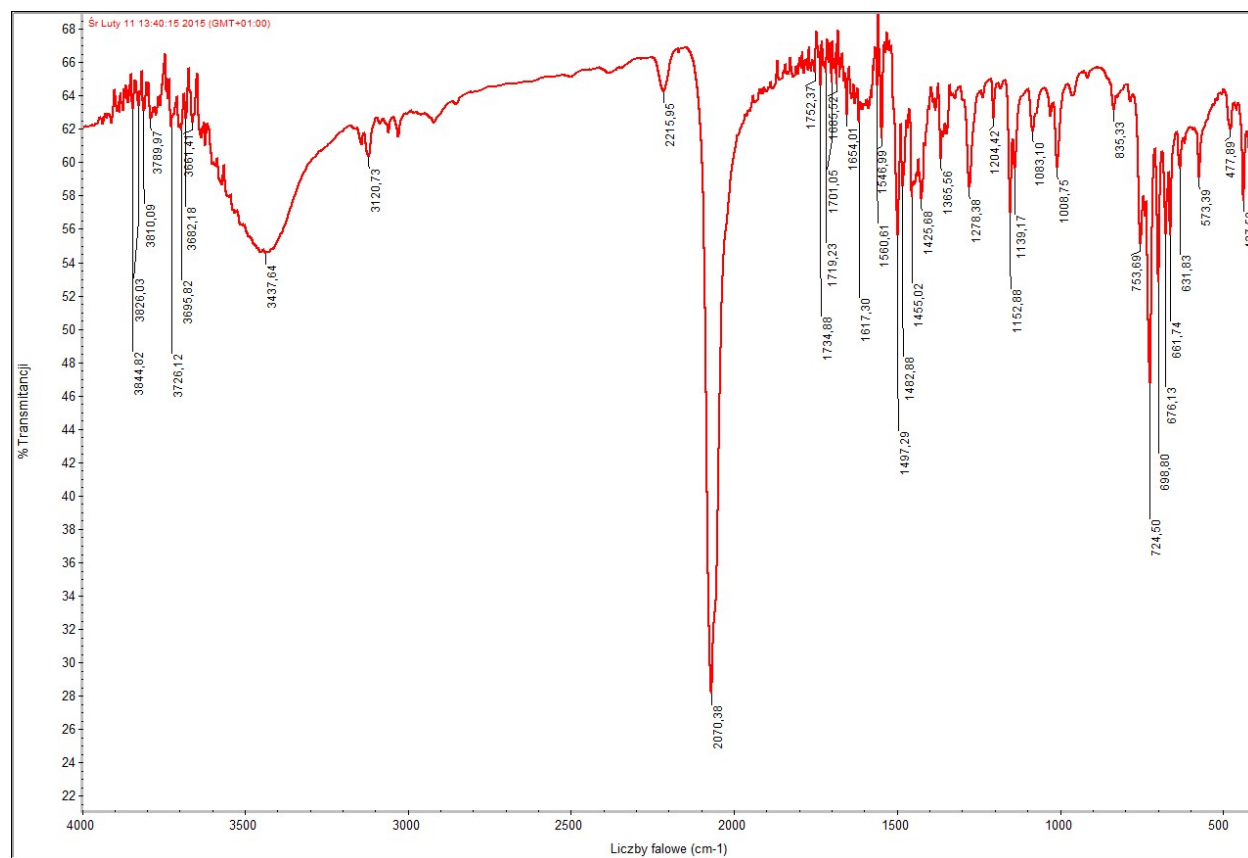


Figure S4. IR spectra of **1**.

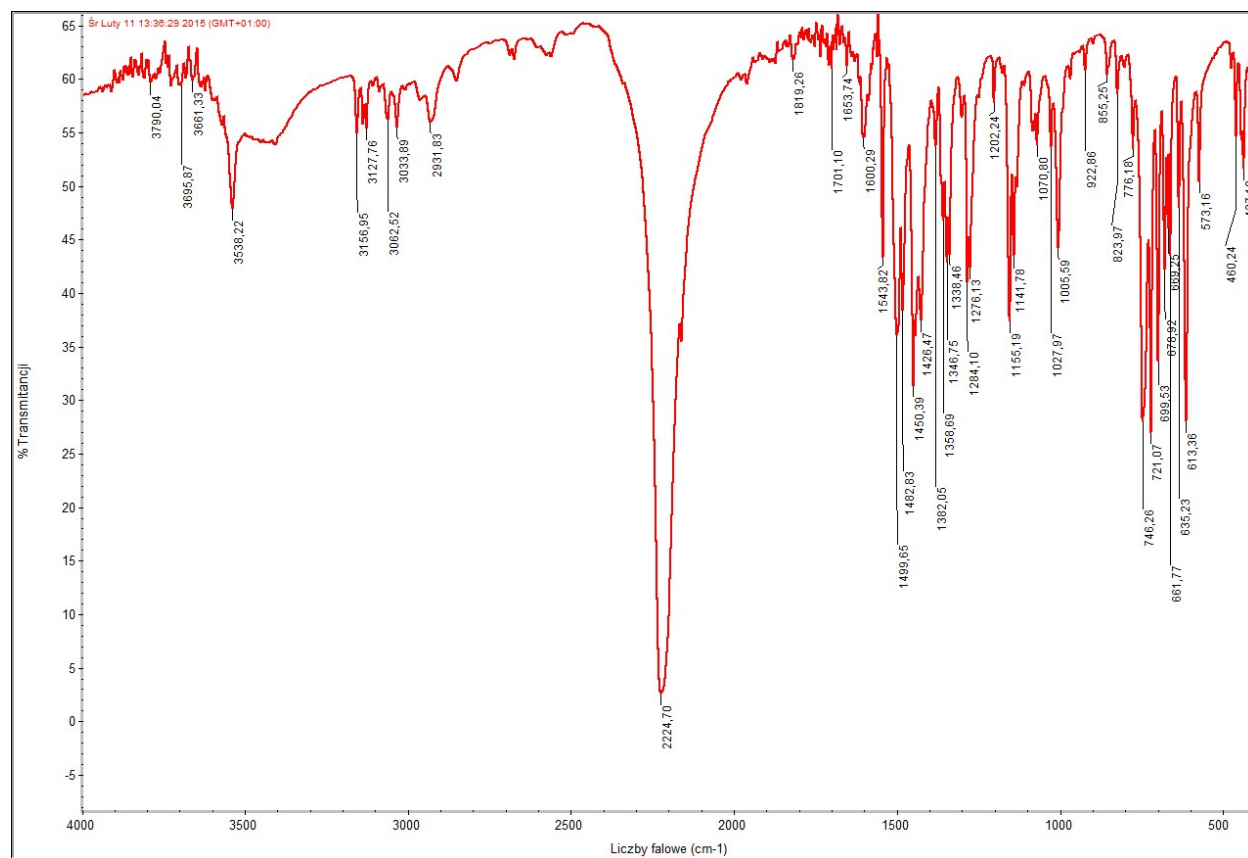


Figure S5. IR spectra of **2**.

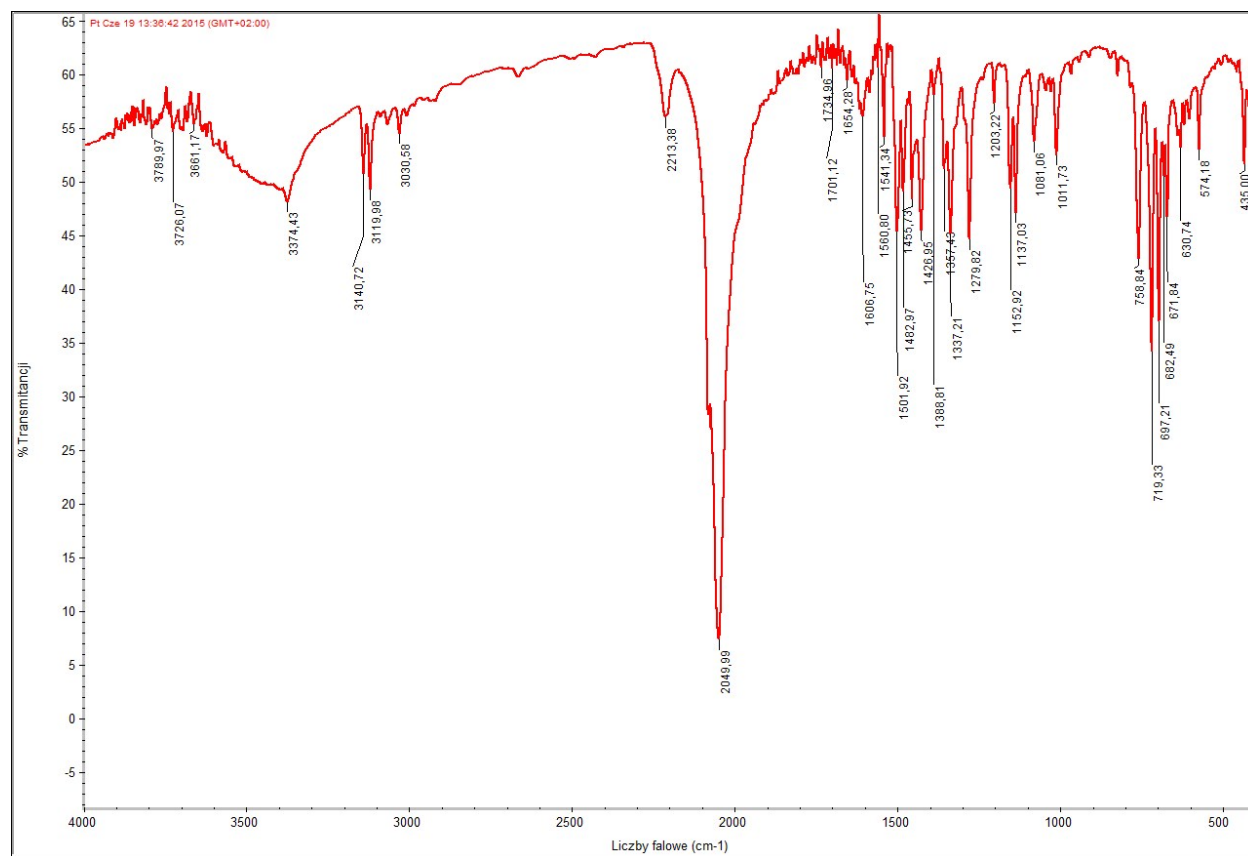


Figure S6. IR spectra of **3**.

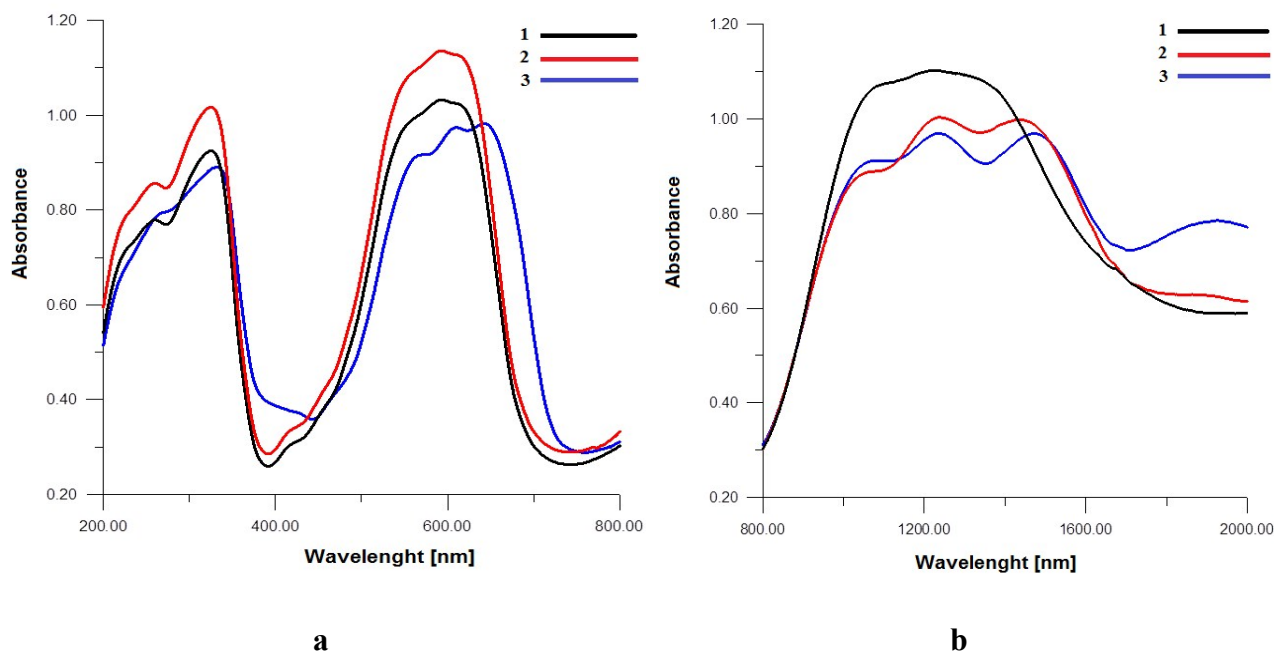


Figure S7. The solid reflectance spectra UV-Vis (a) and NIR (b) of Co(II) complexes

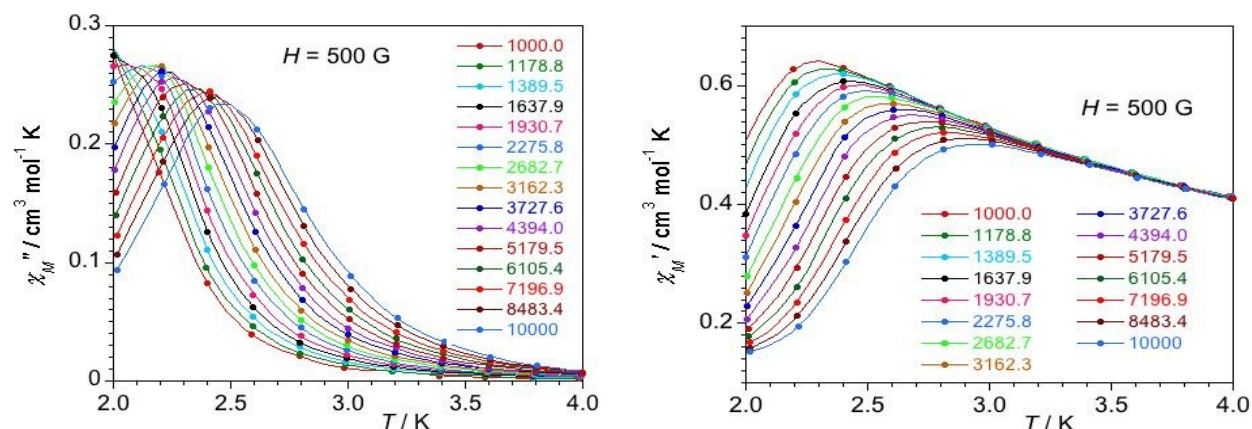


Figure S8. Frequency dependence of the (left) out-of-phase (χ_M'') and (right) in-phase (χ_M') components of the ac susceptibility for **1** under an applied static field of $H_{dc} = 500$ G with a ± 5.0 G oscillating field at frequencies in the range 1000-10000 Hz.

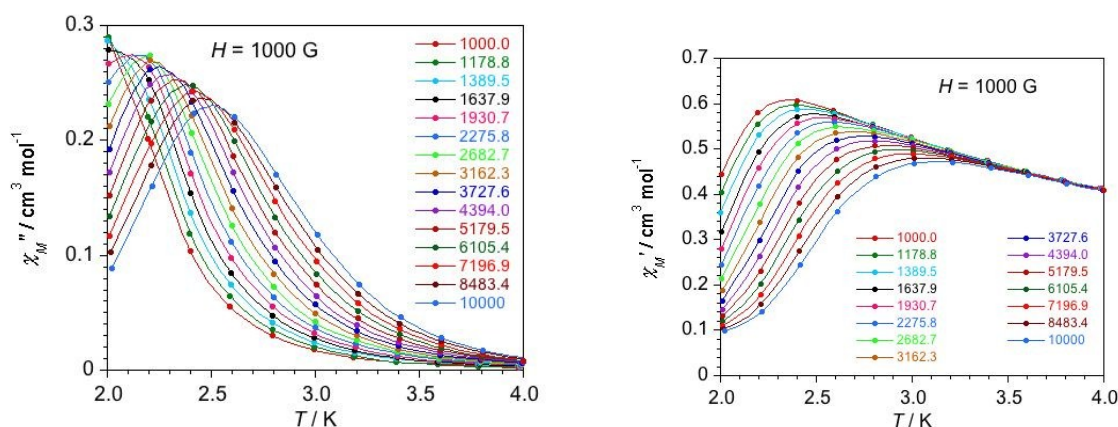


Figure S9. Frequency dependence of the (left) out-of-phase (χ_M'') and (right) in-phase (χ_M') components of the ac susceptibility for **1** under an applied static field of $H_{dc} = 1000$ G with a ± 5.0 G oscillating field at frequencies in the range 1000-10000 Hz.

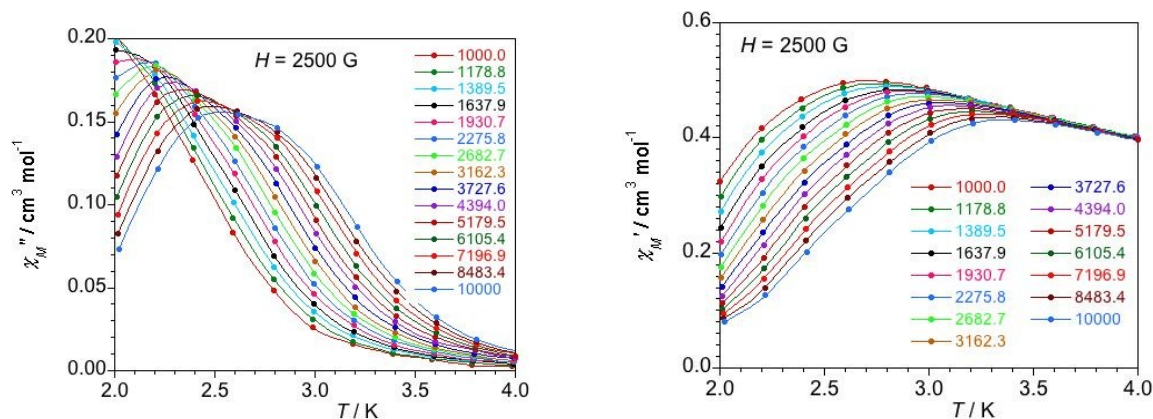


Figure S10. Frequency dependence of the (left) out-of-phase (χ_M'') and (right) in-phase (χ_M') components of the ac susceptibility for **1** under an applied static field of $H_{dc} = 2500$ G with a ± 5.0 G oscillating field at frequencies in the range 1000-10000 Hz.

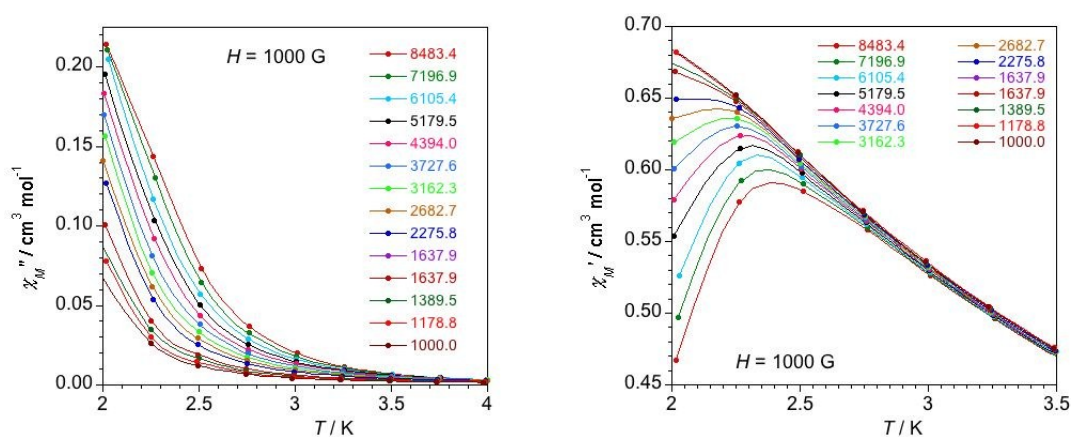


Figure S11. Frequency dependence of the (left) out-of-phase (χ_M'') and (right) in-phase (χ_M') components of the ac susceptibility for **2** under an applied static field of $H_{dc} = 1000$ G with a ± 5.0 G oscillating field at frequencies in the range 1000-10000 Hz.

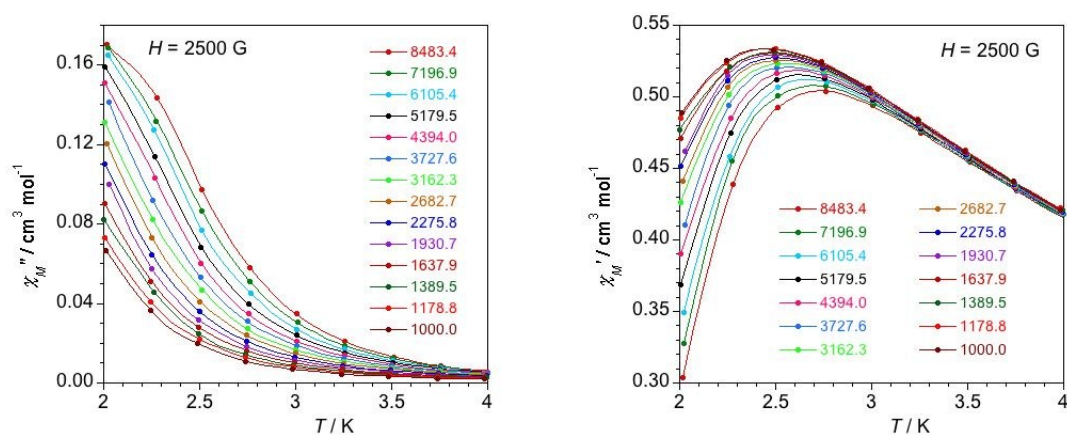


Figure S12. Frequency dependence of the (left) out-of-phase (χ_M'') and (right) in-phase (χ_M') components of the ac susceptibility for **2** under an applied static field of $H_{dc} = 2500$ G with a ± 5.0 G oscillating field at frequencies in the range 1000-10000 Hz.

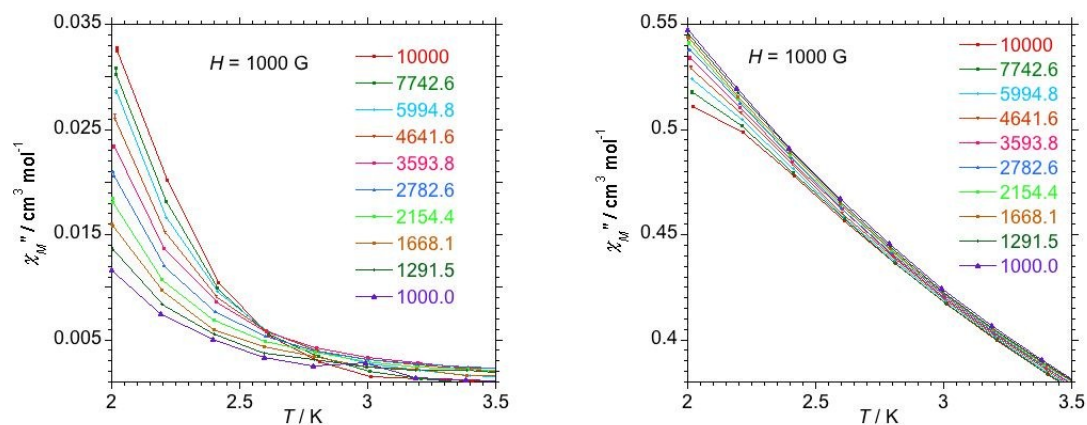


Figure S13. Frequency dependence of the (left) out-of-phase (χ_M'') and (right) in-phase (χ_M') components of the ac susceptibility for **3** under an applied static field of $H_{dc} = 1000$ G with a ± 5.0 G oscillating field at frequencies in the range 1000-10000 Hz.

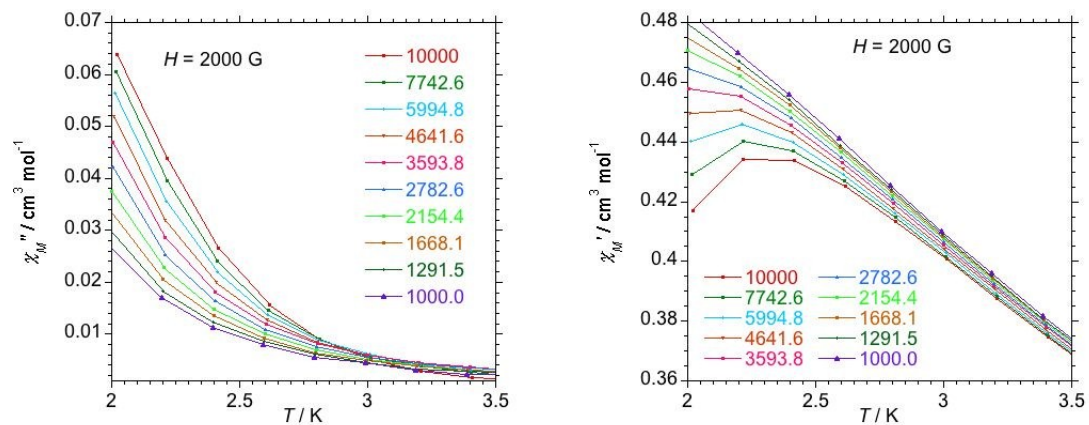


Figure S14. Frequency dependence of the (left) out-of-phase (χ_M'') and (right) in-phase (χ_M') components of the ac susceptibility for **3** under an applied static field of $H_{dc} = 2000$ G with a ± 5.0 G oscillating field at frequencies in the range 1000-10000 Hz.

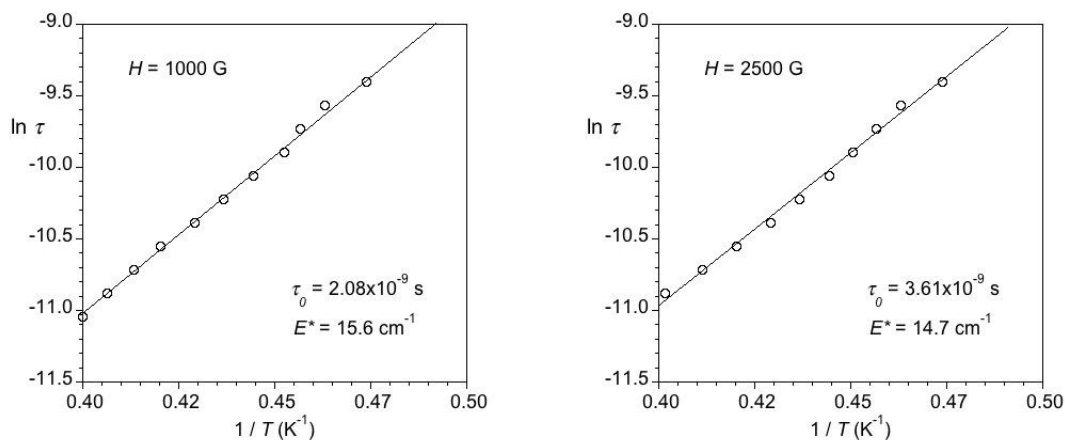


Figure S15. Arrhenius plots for **1** under applied fields of (left) 1000 and (right) 2500 G.

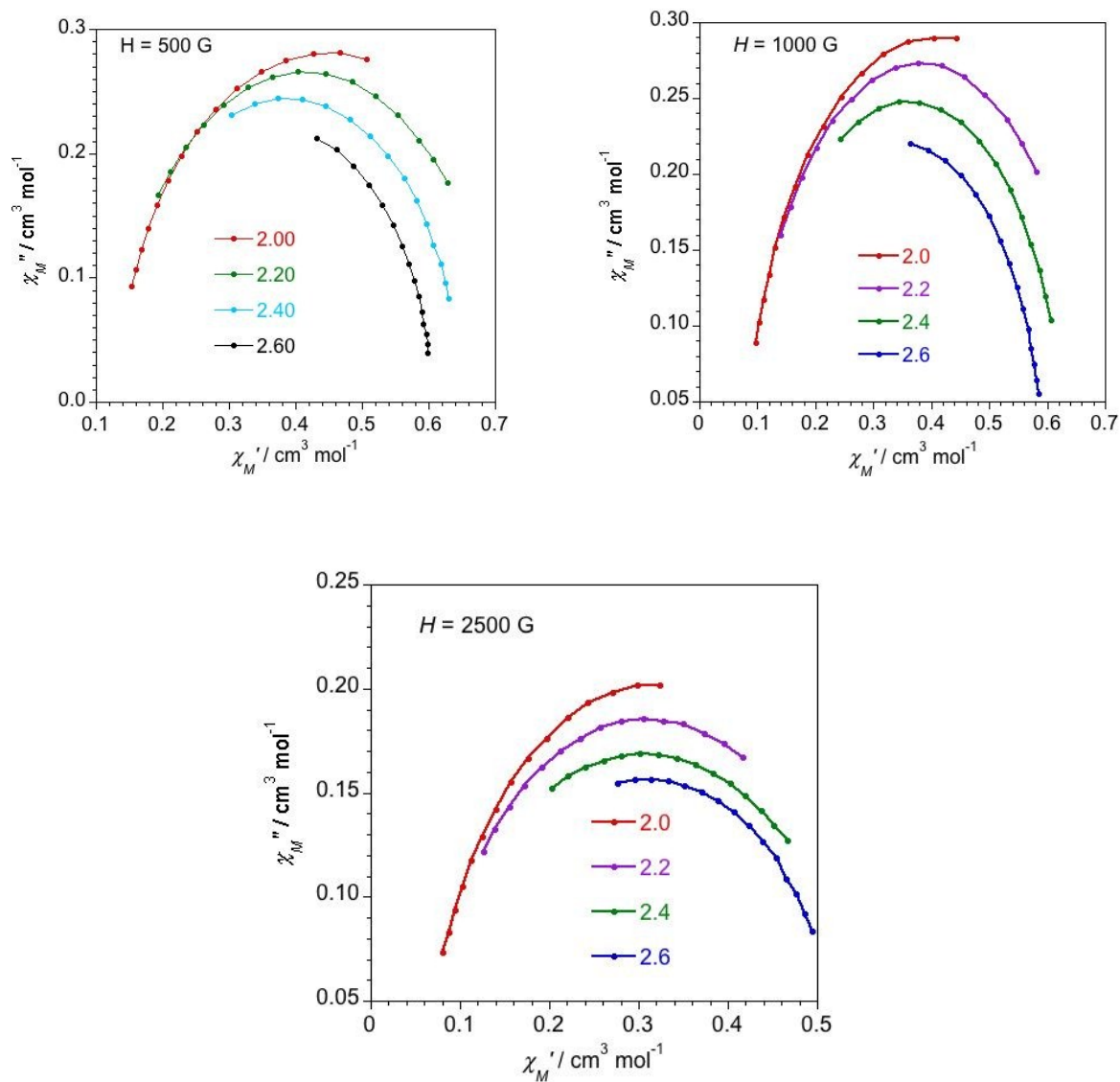


Figure S16. Cole-Cole plots for **1** in the temperature range 2.0-2.6 K at the indicated frequencies and under applied fields of (top) 500, (middle) 1000 and (bottom) 2500 G.

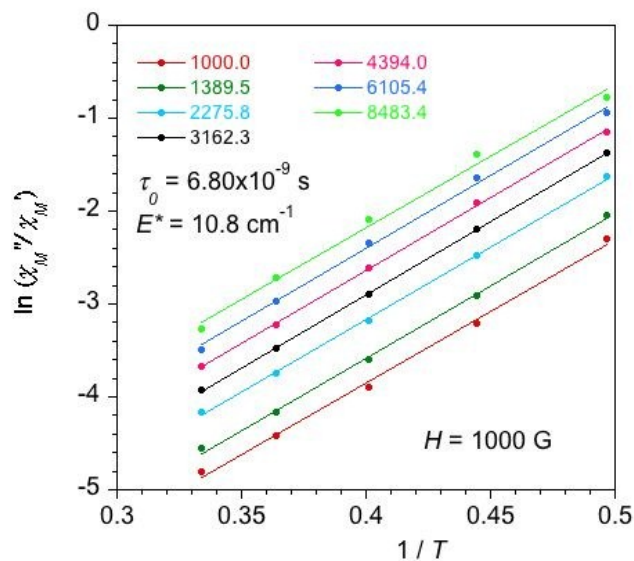


Figure S17. Natural logarithm of the χ_M''/χ_M' ratio vs. $1/T$ for **2** under a dc magnetic field of 1000 G and a ± 5.0 G oscillating field at the indicated frequencies.

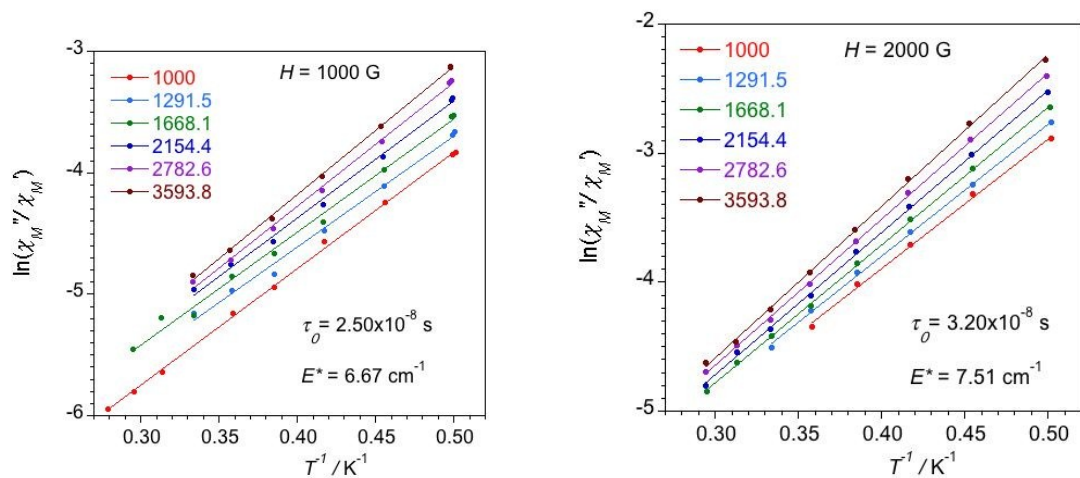


Figure S18. Natural logarithm of the χ_M''/χ_M' ratio vs. $1/T$ for **3** under dc magnetic fields of (left) 1000 and (right) 2000 G and a ± 5.0 G oscillating field at the indicated frequencies

Table S1. Selected bond lengths [Å] and angles [°] for **1-3**

Bond lengths		Bond angles	
1			
Co(1)–N(1)	1.984(6)	N(1)–Co(1)–N(3)	111.3(4)
Co(1)–N(3)	1.961(11)	N(1)–Co(1)–N(3')	114.8(4)
Co(1)–N(3')	2.093(13)	N(1)–Co(1)–N(98)	114.2(3)
Co(1)–N(98)	1.924(6)	N(1)–Co(1)–N(99)	99.5(3)
Co(1)–N(99)	1.948(7)	N(3)–Co(1)–N(98)	119.2(4)
		N(3')–Co(1)–N(98)	95.6(4)
		N(3)–Co(1)–N(99)	98.7(4)
		N(3')–Co(1)–N(99)	122.7(4)
		N(98)–Co(1)–N(99)	110.9(3)
		Co(1)–N(99)–C(99)	164.9(6)
		Co(1)–N(98)–C(98)	169.5(6)
		S(98)–C(98)–N(98)	178.9(6)
		S(99)–C(99)–N(99)	178.7(7)
2			
Co(1)–N(1)	2.012(2)	N(1)–Co(1)–N(3)	105.19(8)
Co(1)–N(3)	2.017(2)	N(1)–Co(1)–N(98)	111.19(9)
Co(1)–N(98)	1.931(2)	N(1)–Co(1)–N(99)	108.58(9)
Co(1)–N(99)	1.939(2)	N(3)–Co(1)–N(98)	113.28(9)
		N(3)–Co(1)–N(99)	105.17(9)
		N(98)–Co(1)–N(99)	112.95(10)
		Co(1)–N(98)–C(98)	165.0(2)
		Co(1)–N(99)–C(99)	170.5(3)
		O(98)–C(98)–N(98)	178.9(3)
		O(99)–C(99)–N(99)	178.7(4)
3			
Co(1)–N(1)	2.011(2)	N(1)–Co(1)–N(1)a	108.25(13)
Co(1)–N(1)a	2.011(2)	N(1)–Co(1)–N(99)	112.34(10)
Co(1)–N(99)	1.951(3)	N(1)–Co(1)–N(99)a	106.83(10)
Co(1)–N(99)a	1.951(3)	N(1)a –Co(1)–N(99)	112.34(10)
		N(99)–Co(1)–N(99)a	110.3(2)
		N(1)a –Co(1)–N(99)a	106.83(10)
		N(97)–N(98)–N(99)	176.4(3)
		Co(1)–N(99)–N(98)	128.3(2)

Symmetry transformations used to generate equivalent atoms: (a) = 1-x,y,1/2-z.

Table S2. UV-VIS-NIR data for compounds **1–3**

Compound	$\lambda_{\max}(\text{cm}^{-1})/(\text{nm})$				B[cm^{-1}]	Dq [cm^{-1}]
	ν_1	ν_2	ν_3	$n \rightarrow \pi^* \pi \rightarrow \pi^*$		
1	7468 (1339) 8156 (1226) 9285 (1077) Average: 8636	16891 (592)	17921 (558)	30769 (325) 39370 (254)	660	859
2	6973 (1434) 8097 (1235) 9560 (1046) Average: 8210	16891 (592)	18148 (551)	30769 (325) 38910 (257)	693	868
3	6793 (1472) 8090 (1236) 9451 (1058) Average 8111	15576 (642)	17825 (561)	30211 (331) 37593 (266)	604	746

Table S3. Short intra- and intermolecular contacts in the structures of **2** and **3**

D—H...A	D—H	H...A	D...A [Å]	D—H...A [°]
2				
C(1)—H(1)...O(98)#a	0.93	2.50	3.1422	126.00
C(5)—H(5B)...O(99)#b	0.93	2.53	3.4259	154.00
C(7)—H(7)...O(99)#b	0.93	2.52	3.3423	147.00
C(18)—H(18)...N(4)#c	0.93	2.60	2.908(4)	100.00
3				
C(4)—H(4A)...N(99)	0.96	2.56	3.406(5)	146.0
C(4)—H(4B)...N(97)#d	0.96	2.50	3.429(4)	163.0

Symmetry transformations used to generate equivalent atoms: #a: $-1+x, y, z$; #b: $-1+x, -1+y, z$; #c: $1-x, 1-y, 1-z$; #d: $x, 1-y, 1/2+z$